

# Tilting the balance towards $d$ -wave in iron-based superconductors

Mario Fink and Ronny Thomale\*

*Institut für Theoretische Physik, Universität Würzburg, Am Hubland, D-97074 Würzburg, Germany*

(Dated: September 3, 2018)

The intricate interplay of interactions and Fermiology can give rise to a close competition between nodeless (e.g.  $s$ -wave) and nodal (e.g.  $d$ -wave) order in electronically driven unconventional superconductors. We analyze how such a scenario is affected by a Zeeman magnetic field  $H_Z$  and temperature  $T$ . In the neighborhood of a zero temperature first order critical point separating a nodal from a nodeless phase, the phase boundary at low  $H_Z$  and/or low  $T$  has a universal line shape cubic in  $H_Z$  or  $T$ , such that the nodal state is stabilized at the expense of the nodeless. We calculate this line shape for a model of competing  $s_{\pm}$ -wave and  $d$ -wave pairing in iron-based superconductors.

*Introduction.* Superconductivity is a quantum many-body state of matter which is a phase-coherent superposition of paired electrons [1]. In order to estimate whether such a state is energetically preferable, we have to consider both the aspects of energy gain due to the formation of the pair condensate as well as the conditions of pairing, i.e., the challenge to overcome the Coulomb repulsion between the electrons. In phonon-mediated superconductors, the interplay of electrons and lattice distortions imply an effective attraction between electrons at appropriate retardation scales [2]; the generically preferred superconducting phase then is an  $s$ -wave state, which optimizes the condensation energy and, at the same time, is least susceptible to disorder. For electronically driven superconductors, the initial challenge is to avoid Coulomb repulsion, which, despite the screening of the long range part of the interactions due to the electron fluid, is still present at small distances. In the cuprates, this is accomplished by  $d$ -wave superconductivity, i.e., through establishing a condensate with finite relative angular momentum of the Cooper pairs. Depending on an itinerant or localized moment point of view, such a condensate is either preferred due to an enhanced  $(\pi, \pi)$  channel of particle hole fluctuations [3] or due to doping an antiferromagnetic Mott insulator [4, 5]. Condensation energy dictates which of the possible  $d$ -wave solutions is preferred: among the in-plane polarized states, the  $d_{x^2-y^2}$ -wave solution is chosen over  $d_{xy}$ -wave, as the Fermi level density of states of the cuprate band structure is smallest along the nodal lines of  $d_{x^2-y^2}$ , which guarantees a minimal loss of condensation energy by the presence of the nodes. Due to the momentum dependence of pairing,  $d$ -wave is more susceptible to disorder than  $s$ -wave [6].

Iron-based superconductors [7] are located such in parameter space that maximizing condensation energy and minimizing Coulomb repulsion are of similar importance. Despite of electron-electron interactions as the apparent dominant role in pairing [8], the interaction scales are weaker than in the cuprates, and multiple Fermi surfaces as well as multiple orbitals that contribute to the pairing significantly complicate the picture [9, 10]. Different theoretical approaches from an itinerant [11–13] and localized moment [14, 15] picture have found

$s$ -wave and  $d$ -wave to be in close competition to each other for iron-based superconductors. The majority of experimental evidence suggests  $s$ -wave superconductivity for most pnictide compounds [16], however, this observation might change as the crystal quality will improve in upcoming waves of refined material synthesis. Some indication along these lines has been recently obtained in  $\text{KFe}_2\text{As}_2$  as the most strongly hole-doped limit of  $\text{K}_x\text{Ba}_{1-x}\text{Fe}_2\text{As}_2$ , where the crystal quality is significantly enhanced through the absence of any Ba content. There, as predicted theoretically [17], thermal conductivity measurements [18, 19] have found strong indication for  $d$ -wave, while the overall situation is still far from settled (see e.g. Ref. 20 and references therein). Recently, Raman scattering has found  $d$ -wave pairing to be of nearly competitive propensity to  $s$ -wave in  $\text{K}_x\text{Ba}_{1-x}\text{Fe}_2\text{As}_2$  crystals of low to intermediate hole doping level  $0.22 < x < 0.7$  [21]. The specific details of this subleading  $d$ -wave state fit the superconducting form factor predicted in [12].

In this Letter, we elaborate on how the competition between an  $s$ -wave and a  $d$ -wave state is affected perturbatively by a Zeeman field  $H_Z$  or temperature  $T$ . As a phenomenological starting point, we place ourselves at a first order zero temperature critical point where we assume a gapped  $s$ -wave and a nodal  $d$ -wave state to be of equal energy density. As partly elaborated on above, such a situation might occur in a multiple Fermi surface scenario with a balanced energetic significance of pairing formation and condensation energy. When a weak Zeeman field is turned on, the  $s$ -wave state will not respond to it since all quasiparticles are gapped. The  $d$ -wave state, however, possesses gapless quasiparticles at the nodes, which are polarized due to the Zeeman field. This gain in magnetic polarization energy makes the  $d$ -wave state preferable, and thus serves as a parameter to tune a phase transition from  $s$ -wave to  $d$ -wave. This similarly applies for finite temperature, where the  $d$ -wave state, in contrast to the  $s$ -wave state, gains free energy through the generation of entropy in the nodal regime. It warrants similarity to the Pomeranchuk effect in  $\text{He}^3$  where the crystal phase is stabilized at finite  $T$  [22, 23].

*Model.* At zero temperature, a singlet superconductor

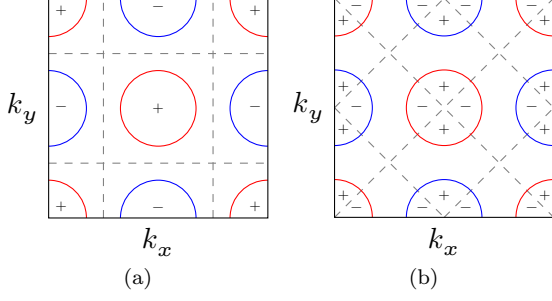


FIG. 1. Schematic plot of the (a)  $s^\pm$ -wave and (b)  $d^\pm$ -wave superconducting gap function for typical electron (blue) and hole pockets (red) in the iron pnictides. "+" and "-" label the sign of the gap functions in the different domains of the Brillouin zone. The zeroes of the gap function (grey dashed lines) do not cross the Fermi surfaces in (a), but yield four nodes for each Fermi pocket in (b). The  $s^\pm$  gap function in (a) corresponds to a second nearest neighbor function of the  $A_{1g}$  representation  $\Delta^{s^\pm}(\mathbf{k}) \propto \cos(k_x)\cos(k_y)$ . The  $d^\pm$  gap function in (b) corresponds to a third nearest neighbor function of the  $B_{1g}$  representation,  $\Delta^{d^\pm}(\mathbf{k}) \propto \cos(2k_x) - \cos(2k_y)$  [12].

subject to a Zeeman field is described by the Hamiltonian

$$H = \sum_{\mathbf{k}, \sigma, \sigma'} (\varepsilon(\mathbf{k}) - \mu_B H_Z \sigma^z_{\sigma, \sigma'}) c_{\mathbf{k}, \sigma}^\dagger c_{\mathbf{k}, \sigma'} + \frac{1}{2} \sum_{\mathbf{k}, \sigma, \sigma'} \left( \Delta_{\sigma, \sigma'}(\mathbf{k}) c_{\mathbf{k}, \sigma}^\dagger c_{-\mathbf{k}, \sigma'}^\dagger + \text{h.c.} \right), \quad (1)$$

where  $\varepsilon(\mathbf{k})$  is the kinetic term of the electrons,  $\Delta_{\sigma, \sigma'}(\mathbf{k}) = i\Delta(\mathbf{k})\sigma^y_{\sigma, \sigma'}$ , and  $\sigma^y, \sigma^z$  denote the Pauli matrices. The orbital magnetic field contribution be weak in comparison to the Zeeman term, e.g. as accomplished by an in-plane field [24] in a quasi two-dimensional crystal [25]. For  $H_Z = 0$  and  $T = 0$ , our phenomenological ansatz assumes energy densities  $e_s = e_d$  of an  $s$ -wave and a  $d$ -wave state.

As a specific competing candidate state in materials such as the pnictides, we consider extended  $s$ -wave ( $s_\pm$ )  $\Delta^{s^\pm}(\mathbf{k}) = \Delta_s (\cos(k_x)\cos(k_y))$  [26, 27] and extended  $d$ -wave  $\Delta^{d^\pm}(\mathbf{k}) = \Delta_d (\cos(2k_x) - \cos(2k_y))$  [12] (Fig. 1). This choice is motivated by recent Raman scattering experiments on K-doped Ba-122 where both the leading and subleading superconducting order can be detected, rendering the  $s_\pm$ -wave and  $d_\pm$ -wave states close competitors [21]. In our argument to follow, it is irrelevant which type of  $d$ -wave or  $s$ -wave is realized. The only assumption is that the anisotropy in the  $s$ -wave state be small enough to provide a minimal quasiparticle gap  $\Delta_s > \mu_B H_Z$  (the reduction of  $s^\pm$ -wave gap anisotropy, which by itself can be vital to explaining the experimental data in iron pnictides [28], is often caused by disorder [29]), and that the  $d$ -wave state is nodal. The latter is a property protected by symmetry, as long as the nodal lines intersect with at least one Fermi pocket.

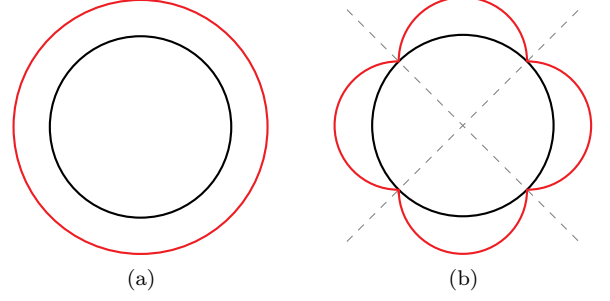


FIG. 2. (a) Schematic representation of the quasiparticle spectral gap (solid red line) (3) for an ideal  $s$ -wave scenario  $\Delta(\mathbf{k}) = \Delta_s$  displaying a finite gap along the entire Fermi surface (solid black line). (b) In contrast, the  $d$ -wave gap exhibits nodes (dashed lines) where the gap vanishes.

*Bogoliubov quasiparticles.* To obtain the SC quasiparticle spectrum, we represent (1) by its Bogoliubov-de Gennes (BdG) form, i.e. we employ Nambu spinor  $\vec{C}_{\mathbf{k}}^\dagger = (c_{\mathbf{k}, \uparrow}^\dagger, c_{\mathbf{k}, \downarrow}^\dagger, c_{-\mathbf{k}, \uparrow}, c_{-\mathbf{k}, \downarrow})$  notation and obtain

$$\mathcal{H} = \frac{1}{2} \sum_{\mathbf{k}} \vec{C}_{\mathbf{k}}^\dagger \begin{pmatrix} \varepsilon(\mathbf{k}) - \mu_B H_Z \sigma^z & i\Delta(\mathbf{k})\sigma^y \\ -i\Delta^*(\mathbf{k})\sigma^y & -\varepsilon(\mathbf{k}) + \mu_B H_Z \sigma^z \end{pmatrix} \vec{C}_{\mathbf{k}}. \quad (2)$$

The eigenvalue spectrum of (2) is given by

$$E^{\pm, \pm}(\mathbf{k}) = \pm \mu_B H_Z \pm \sqrt{\varepsilon(\mathbf{k})^2 + |\Delta(\mathbf{k})|^2}, \quad (3)$$

where the two binary indices label the up/down spin (later denoted  $\sigma$ ) and Bogoliubov particle/hole character, respectively. The eigenstates are given by

$$\begin{aligned} \psi_{\mathbf{k}}^{\dagger, (-, \pm)} &= \Delta(\mathbf{k}) c_{\mathbf{k}, \uparrow}^\dagger - \left( \varepsilon(\mathbf{k}) \mp \sqrt{\varepsilon^2(\mathbf{k}) + |\Delta(\mathbf{k})|^2} \right) c_{-\mathbf{k}, \downarrow} \\ \psi_{\mathbf{k}}^{\dagger, (+, \pm)} &= \Delta(\mathbf{k}) c_{\mathbf{k}, \downarrow}^\dagger + \left( \varepsilon(\mathbf{k}) \mp \sqrt{\varepsilon^2(\mathbf{k}) + |\Delta(\mathbf{k})|^2} \right) c_{-\mathbf{k}, \uparrow}. \end{aligned} \quad (4)$$

*Quasiparticle magnetization.* Assume  $k_B T \approx 0$  to be the smallest of all energy scales, and consider the spectrum (3) in the case of  $\Delta(\mathbf{k}) = \Delta^{s_\pm, d_\pm}(\mathbf{k})$  for one representative Fermi pocket (Fig. 2): for the case of  $s_\pm$ -wave in Fig. 2a,  $\Delta(\mathbf{k}) \approx \Delta_s$ . For  $\mu_B H_Z < \Delta_s$ , the Zeeman field has a negligible effect on the spectrum because the binding energy of the singlet pair is larger than the applied field. For  $d_\pm$ -wave, however, while gapped by  $\Delta(\mathbf{k}) \approx \Delta_d$  in the anti-nodal regime, there is a nodal regime  $\Delta(\mathbf{k}) \approx 0$  illustrated in Fig. 3b where the quasiparticles will respond to the Zeeman field [24]. We expand the quasiparticle dispersion (3) around the nodal regime in momentum space at  $\mathbf{k}_F^*$ . Define

$$v_F \equiv \left. \frac{\partial E(\mathbf{k})}{\partial k_\perp} \right|_{\mathbf{k}=\mathbf{k}_F^*}, \quad v_\Delta \equiv \left. \frac{\partial E(\mathbf{k})}{\partial k_\parallel} \right|_{\mathbf{k}=\mathbf{k}_F^*}, \quad (5)$$

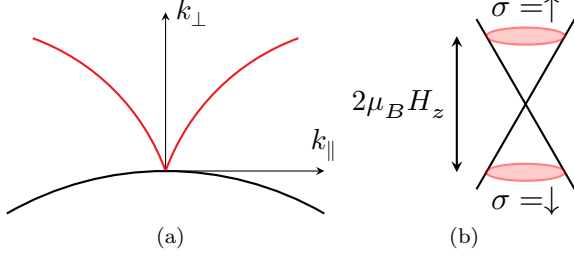


FIG. 3. (a) In the vicinity of a node, the  $d$ -wave spectrum features a linear momentum dependence characterized by  $k_{\perp}$  and  $k_{\parallel}$ . (b) In the presence of a finite magnetic field, the point-like Fermi surface of the Bogoliubov cone splits into two elliptic Fermi surfaces for opposite spins.

where  $k_{\perp}$  and  $k_{\parallel}$  are the momenta perpendicular and tangential to the Fermi surface of  $\varepsilon(\mathbf{k})$  (Fig. 3a). The dispersion takes the form of an elliptic Dirac cone

$$E(\mathbf{k})|_{\mathbf{k} \approx \mathbf{k}_F^*} = v_F k_{\perp} + v_{\Delta} k_{\parallel} \quad . \quad (6)$$

Due to  $H_Z$ , the Fermi levels of spin  $\uparrow$  and  $\downarrow$  quasiparticles shift against each other, and a Fermi pocket emerges, with its surface given by the elliptic equation

$$(k_{\perp} - k_{F,\perp}^*)^2 v_F^2 + (k_{\parallel} - k_{F,\parallel}^*)^2 v_{\Delta}^2 = \mu_B^2 H_Z^2 \quad . \quad (7)$$

Computing the magnetization from there, without loss of generality, we constrain ourselves to the spin  $\uparrow$  species. The number of particles in a given volume  $\mathcal{V}$  is given by the area enclosed by the Fermi surface (7)

$$\begin{aligned} N_{\uparrow} &= \langle FS | n_{\mathbf{k},\uparrow} | FS \rangle \\ &= \frac{\mathcal{V}}{(2\pi)^2} \pi \frac{\mu_B^2 H_Z^2}{v_F v_{\Delta}} \quad . \end{aligned} \quad (8)$$

From the density  $n_{\uparrow}(E) = \frac{1}{4\pi} \frac{E^2}{v_F v_{\Delta}}$ , we obtain the energy density of states  $\rho(E) = \frac{\partial n_{\uparrow}}{\partial E} = \frac{1}{2\pi} \frac{E}{v_F v_{\Delta}}$ . Considering both spin  $\uparrow$  and  $\downarrow$  contributions, we eventually obtain the quasiparticle magnetization density

$$\begin{aligned} m &= \mu_B (n_{\uparrow} - n_{\downarrow}) = 2\mu_B \int_0^{\mu_B H_Z} \rho(E) dE \\ &= \frac{\mu_B}{2\pi} \frac{\mu_B^2 H_Z^2}{v_F v_{\Delta}} \quad . \end{aligned} \quad (9)$$

Assuming we had started from an equal energy density for  $s$ -wave and  $d$ -wave, the Zeeman field hence yields a *preference* for  $d$ -wave according to

$$e_d - e_s = -m H_Z = -N_n \frac{(\mu_B H_Z)^3}{2\pi v_F v_{\Delta}} \quad , \quad (10)$$

where  $N_n$  denotes the total number of nodes induced by the  $d$ -wave state on the multi-pocket Fermi surface.

*Quasiparticle entropy.* Assume  $H_Z \approx 0$  and finite temperature  $k_B T < \Delta_s$ . The free energy density is given by

$f = u - Ts = -k_B T / N \ln \mathcal{Z}$ , where  $u$  denotes the inner energy density,  $T$  the temperature,  $s$  the entropy per particle, and  $\mathcal{Z}$  the (grand) canonical partition function. The latter be denoted by

$$\mathcal{Z} = \sum_{\{|\Psi\rangle\}} e^{-\beta E_{|\Psi\rangle}} = \prod_{\mathbf{k}\sigma} \left( 1 + e^{-\beta E_{\sigma,+}(\mathbf{k})} \right) \quad , \quad (11)$$

with  $\frac{1}{\beta} = k_B T$ , spin index  $\sigma = \pm$ , many-particle state  $|\Psi\rangle$ , and the corresponding energy  $E_{|\Psi\rangle}$  constructed from the single-particle states (4) and the quasiparticle energy  $E_{\sigma,+}(\mathbf{k})$  given by (3), as we only consider the particle-type Bogoliubov branch. We set  $e_d = e_s$  such that for the relative change in free energy density  $f_d - f_s$ , the inner energy does not enter. The nodal regime of the  $d$ -wave state then is the only relevant contribution to the change of  $f_d - f_s$  at low temperatures. Since  $f$  depends only on the momentum  $\mathbf{k}$  through the energy  $E(\mathbf{k})$ , we express it by means of the density of states  $\rho_{\sigma,+}(E(\mathbf{k}))$  to find

$$f = -k_B T \sum_{\sigma} \int_{-\infty}^{+\infty} \rho_{\sigma,+}(E) \ln \left( 1 + e^{-\beta E_{\sigma,+}} \right) dE \quad (12)$$

Due to the discontinuity of  $\rho_{\sigma,+}(E)$  at the band edge, we have to include the boundary terms upon partial integration. The boundary terms, however, may be neglected for  $\beta \gg 1$ , which, together with  $f_s \approx 0$  in this limit, leaves us with

$$f_d - f_s \stackrel{\beta \gg 1}{\approx} - \sum_{\sigma} \int_0^{E_{\max}} \frac{\Upsilon_{\sigma,+}(E)}{e^{\beta E_{\sigma,+}} + 1} dE \quad , \quad (13)$$

where  $\rho_{\sigma,+}(E) = \frac{d\Upsilon_{\sigma,+}(E)}{dE}$  and  $E_{\max} = \limsup_{\mathbf{k} \in \text{BZ}} E_{\sigma,+}(\mathbf{k})$ . We are interested in the low-temperature behavior of  $f_d$ , which is why we are allowed to model the density of states by a linear function along with (6), i.e.  $\rho_{\sigma,+}(E) = \alpha E_{\sigma,+}$  such that  $\Upsilon_{\sigma,+}(E) = \frac{\alpha}{2} E_{\sigma,+}^2$ . This reduces our task to solving the Fermi-Dirac integral

$$\frac{\alpha}{2} \int_0^{E_{\max}} \frac{E^2}{e^{\beta E} + 1} dE = \frac{\alpha}{2} \frac{1}{\beta^3} \int_0^{\beta E_{\max}} \frac{x^2}{e^x + 1} dx \quad . \quad (14)$$

It already shows that the change in free energy density has the low-temperature behavior  $f_d - f_s \propto -T^3$ . The integral is solved by the integrand's primitive [30, 31]

$$\Xi(x) = \frac{x^3}{3} - x^2 \ln(1 + e^x) - 2x \text{Li}_2(-e^x) + 2 \text{Li}_3(-e^x) \quad , \quad (15)$$

where  $\text{Li}_i(x)$  denotes the polylogarithm [32]. The result may be easily checked using  $\frac{d}{dx} \text{Li}_s(x) = \frac{1}{x} \text{Li}_{s-1}(x)$  and  $\text{Li}_1(x) = -\ln(1 - x)$ . The integral in (14) gives

$$\Xi(\beta E_{\max}) - \Xi(0) \approx -2 \text{Li}_3(-1) = 2\eta(3) \quad , \quad (16)$$

where we neglect  $\Xi(\beta E_{\max})$  for small temperatures since  $\lim_{x \rightarrow \infty} \Xi(x) = 0$ . We express the polylogarithm in

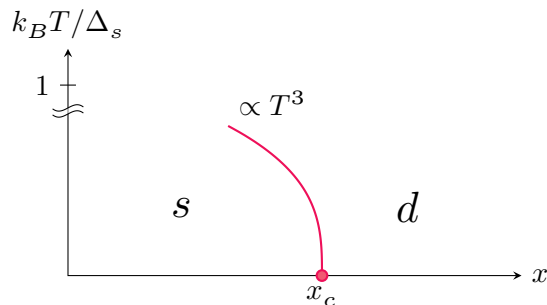


FIG. 4. Sketch of the phase boundary between a competing gapped  $s$ -wave and nodal  $d$ -wave state as a function of tuning parameter  $x$  and temperature  $T$ . Emanating from a first order quantum critical point at  $x_c$ , there is a universal cubic trajectory for temperatures below the gap scale  $\Delta_s$ .

terms of the Dirichlet  $\eta$ -function, which in turn is written in terms of the Riemann  $\zeta$ -function  $\eta(s) = (1 - 2^{1-s})\zeta(s)$ . Having thus fixed the exact prefactor, we find

$$f_d - f_s \stackrel{\beta \gg 1}{\approx} -\frac{3}{2}\alpha\zeta(3)(k_B T)^3, \quad (17)$$

with  $\zeta(3) \approx 1.20206$  (Apéry's constant), and the universal cubic phase boundary shape depicted in Fig. 4. This finding is calculated for one single node, and would have to be multiplied by  $N_n$  to account for the total number of nodes. In (17),  $\alpha$  is the non-universal coefficient which is sensitive to the details of the microscopic system. To calculate an explicit example, we take the one-band Hubbard model  $\epsilon(\mathbf{k}) = -2t(\cos(k_x) + \cos(k_y)) - \mu$  with a nearly circular Fermi pocket for  $t = 1.0$ ,  $\mu = -1.9$ . Its density of states at the nodes (which may be derived by means of  $v_F$  and  $v_\Delta$  in Eq. 5) gives  $\alpha \approx 1.58$ .

*Conclusion.* At the latest since the discovery of the iron pnictides, materials with competitive unconventional nodal and nodeless superconducting pairing tendencies have established an intricate problem to be further studied experimentally and theoretically. We have shown that the perturbative Zeeman-magnetic and entropic response of nodal quasiparticles pave the way to tilt the thermodynamic balance in favor of the nodal, in our case  $d$ -wave, superconducting state by a term which is cubic in the perturbation parameter, i.e. either  $H_Z$  or  $T$ . In the neighborhood of a zero temperature first order critical point between the nodal and the nodeless state, this gives rise to a universal cubic phase transition line shape in favor of the nodal state. Whether this contribution can yield an observable magnetically or entropically induced superconducting phase transition crucially relies on a careful material design as well as the detailed tunability of system parameters towards such a critical point. From a broader perspective, iron-based superconductors are not the only class of materials displaying comparable superconducting pairing tendencies towards a nodal and a nodeless state. For instance, the nodeless chiral  $p$ -wave

state predicted for strontium ruthenate [33] is challenged by a nodal  $d$ -wave state, where unfortunately the possibly strongly anisotropic gap profile makes it hard to discriminate between both superconducting states [34, 35]. It is likely, however, that the  $d$ -wave state eventually has to win beyond a critical amount of strain [36], rendering the latter an ideal experimental tuning parameter towards the critical point regime between a nodal and nodeless superconducting state we have envisioned in this work.

We thank S. A. Kivelson, A. V. Chubukov, P. Hirschfeld, A. Mackenzie, I. I. Mazin, S. Raghu, and D. Scalapino for stimulating discussions. This work was supported by DFG-SPP 1458, DFG-SFB 1170 (project B04), and ERC-StG-336012-TOPOLECTRICS.

---

\* rthomale@physik.uni-wuerzburg.de

- [1] J. R. Schrieffer, *Theory of Superconductivity* (Benjamin/Addison Wesley, New York, 1964).
- [2] J. Bardeen, L. N. Cooper, and J. R. Schrieffer, Phys. Rev. **108**, 1175 (1957).
- [3] W. Kohn and J. M. Luttinger, Phys. Rev. Lett. **15**, 524 (1965).
- [4] P. W. Anderson, Science **235**, 1196 (1987).
- [5] P. A. Lee, N. Nagaosa, and X.-G. Wen, Rev. Mod. Phys. **78**, 17 (2006).
- [6] P. W. Anderson, J. Phys. Chem. Solids **11**, 26 (1959).
- [7] Y. Kamihara, T. Watanabe, M. Hirano, and H. Hosono, Journal of the American Chemical Society **130**, 3296 (2008), PMID: 18293989.
- [8] L. Boeri, O. V. Dolgov, and A. A. Golubov, Phys. Rev. Lett. **101**, 026403 (2008).
- [9] P. J. Hirschfeld, M. M. Korshunov, and I. I. Mazin, Reports on Progress in Physics **74**, 124508 (2011).
- [10] A. V. Chubukov, Annual Review of Condensed Matter Physics **3**, 57 (2012).
- [11] K. Kuroki *et al.*, Phys. Rev. Lett. **101**, 087004 (2008).
- [12] R. Thomale, C. Platt, J. Hu, C. Honerkamp, and B. A. Bernevig, Phys. Rev. B **80**, 180505 (2009).
- [13] S. Graser, T. Maier, P. Hirschfeld, and D. Scalapino, New Journal of Physics **11**, 025016 (2009).
- [14] Q. Si and E. Abrahams, Phys. Rev. Lett. **101**, 076401 (2008).
- [15] K. Seo, B. A. Bernevig, and J. Hu, Phys. Rev. Lett. **101**, 206404 (2008).
- [16] G. R. Stewart, Rev. Mod. Phys. **83**, 1589 (2011).
- [17] R. Thomale, C. Platt, W. Hanke, J. Hu, and B. A. Bernevig, Phys. Rev. Lett. **107**, 117001 (2011).
- [18] J.-P. Reid *et al.*, Physical Review Letters **109**, 087001 (2012).
- [19] A. F. Wang *et al.*, Phys. Rev. B **89**, 064510 (2014).
- [20] C. Platt, G. Li, M. Fink, W. Hanke, and R. Thomale, physica status solidi (b) **254**, 1600350 (2017), 1600350.
- [21] T. Böhm *et al.*, arXiv:1703.07749.
- [22] I. Pomeranchuk, JETP **20**, 919 (1950).
- [23] R. C. Richardson, Rev. Mod. Phys. **69**, 683 (1997).
- [24] K. Yang and S. L. Sondhi, Phys. Rev. B **57**, 8566 (1998).
- [25] Orbital magnetic field effects of a nodal superconductor generically dominate over the Zeeman term at weak field

- strength for a field orientation perpendicular to the 2D plane. The Volovik effect [37] then predicts a  $\propto \sqrt{H}$  scaling of the induced density of states, as opposed to the  $\propto H$  scaling for the Zeeman term.
- [26] I. I. Mazin, D. J. Singh, M. D. Johannes, and M. H. Du, *Phys. Rev. Lett.* **101**, 057003 (2008).
  - [27] F. Wang, H. Zhai, Y. Ran, A. Vishwanath, and D.-H. Lee, *Phys. Rev. Lett.* **102**, 047005 (2009).
  - [28] R. Thomale, C. Platt, W. Hanke, and B. A. Bernevig, *Phys. Rev. Lett.* **106**, 187003 (2011).
  - [29] V. Mishra *et al.*, *Phys. Rev. B* **79**, 094512 (2009).
  - [30] M. H. Lee, *Journal of Mathematical Physics* **36**, 1217 (1995).
  - [31] M. Morales, arXiv:0909.3653.
  - [32] M. Abramowitz and I. A. Stegun, New York 361 (1972).
  - [33] T. M. Rice and M. Sigrist, *Journal of Physics: Condensed Matter* **7**, L643 (1995).
  - [34] Q. H. Wang *et al.*, *EPL (Europhysics Letters)* **104**, 17013 (2013).
  - [35] E. Hassinger *et al.*, *Phys. Rev. X* **7**, 011032 (2017).
  - [36] C. W. Hicks *et al.*, *Science* **344**, 283 (2014).
  - [37] G. E. Volovik, *JETP Lett.* **58**, 457 (1993).